Polymer Chemistry

Synthesis and Self-Assembly of Diphenylalanine–Tetraphenylethylene Hybrid Monomer and RAFT Polymers with Aggregation-Induced Emission

Journal:	*Polymer Chemistry*
Manuscript ID	PY-ART-12-2022-001602.R1
Article Type:	Paper
Date Submitted by the Author:	20-Feb-2023
Complete List of Authors:	Yonenuma, Ryo; Yamagata Daigaku Daigakuin Yuki Zairyo System Kenkyuka Mori, Hideharu; Yamagata Daigaku Daigakuin Yuki Zairyo System Kenkyuka

ARTICLE

Synthesis and Self-Assembly of Diphenylalanine-Tetraphenylethylene Hybrid Monomer and RAFT Polymers with Aggregation-Induced Emission

Received 00th January 20xx,
Accepted 00th January 20xx

DOI: 10.1039/x0xx00000x

Ryo Yonenuma,[a] Hideharu Mori[a]*

A hybrid monomer consisting of diphenylalanine with the self-assembling ability and tetraphenylethylene (TPE) with aggregation-induced emission (AIE) properties was synthesized and employed for reversible addition-fragmentation chain transfer polymerization. The diphenylalanine–TPE hybrid monomer (APhePheTPE) self-assembled into helical nanoribbons and fiber-like structures and exhibited AIE properties with blue emissions, which originated from the aggregation of TPE units by tuning the water fraction in the tetrahydrofuran/water mixtures. The APhePheTPE revealed the formation of β-sheet structures and aggregation-induced circular dichroism (AICD) by achiral TPE units via interactions with diphenylalanine moieties. The APhePheTPE homopolymers showed the feasibility of forming stable assembled structures, such as rod-shaped structures and nanofibers, with characteristic molecular weight-dependent emissions and AIE properties. This study revealed the potential of the polymerizable diphenylalanine–TPE hybrid monomer as a building block for the development of chiral AIE hybrid polymers with the ability to form various self-assembled structures and characteristic AIE and AICD properties.

Introduction

Diphenylalanine is an aromatic dipeptide composed of two phenylalanine and is of great interest as a simple and versatile building block. This dipeptide exhibits a unique intrinsic ability to self-assemble into various nanostructures, such as nano/microtubes,[1-4] nanofibers, and nanowires.[3,5] Manipulation of various non-covalent interactions (such as aromatic stacking, hydrogen bonding, and electrostatic interactions) and sample preparation conditions (such as solvent/co-solvent polarities) are crucial for controlling the intrinsic self-assembly of dipeptide derivatives. Diphenylalanine also functions as a core recognition portion of β-amyloid in Alzheimer's disease via hydrophobic interactions.[1] Thus, the diphenylalanine motif offers a unique direction in designing new bio-inspired nanomaterials with superior mechanical and physical properties. An increasing number of potential applications have been observed in various fields, such as templates,[1] gels,[6,7] piezoelectrics,[8,9] antimicrobial activity,[10,11] and biosensors.[12,13]

As an efficient approach for developing functional polymers with bio-inspired nanostructures, the merging of the attractive features of diphenylalanine with the advantages of synthetic polymers has gained significant attention. Margel et al. reported the synthesis of hydrophobic dipeptide (*N*-acryloyl-L,L-diphenylalanine methyl ester)-based polymeric nanoparticles, which showed biocompatibility and inhibition of amyloid-β fibrillation.[14] Jeong et al. reported substantial improvement in the physical properties of polymeric gels consisting of ethylene glycol and propylene glycol triblock copolymers by introducing diphenylalanine moieties into the end groups.[15] Our previous study also demonstrated the synthesis of homo- and copolymers with characteristic self-assemblies and thermoresponsiveness via reversible addition-fragmentation chain-transfer (RAFT) polymerization of a dipeptide-containing acrylamide (*N*-acryloyl-L,L-diphenylalanine, APhePheOH).[16] Knight et al. recently demonstrated the RAFT synthesis of amphiphilic copolymers containing hydrophilic monomers and a hydrophobic diphenylalanine acrylamide, along with the formation of globule and β-sheet-like structures derived from the dipeptide side chain.[17] Other examples of diphenylalanine-polymer conjugates include the hybrid copolymers containing polylactide,[18,19] polyurethane,[20] and DNA,[21] as well as nanoobjects prepared via polymerization-induced self-assembly of a methacrylate with diphenylalanine-containing tripeptide.[22,23]

Aggregation-induced emission (AIE) molecules, such as hexaphenylsilole and tetraphenylethylene (TPE), have been extensively explored, which exhibit no emission in the molecularly dissolved states but strong emission in the aggregation or solid state.[24-28] These molecules have been widely used in bioimaging,[29] sensing,[30] and theragnostic applications[26] owing to their unique AIE characteristics and structural diversity. The combination of AIE molecules with self-assembling motifs via molecular modifications is promising in

[a] *Department of Organic Material Science, Graduate School of Organic Materials Science, Yamagata University, 4-3-16, Jonan, Yonezawa City, Yamagata Prefecture 992-8510, Japan, E-mail: h.mori@yz.yamagata-u.ac.jp.*
Electronic Supplementary Information (ESI) available. See DOI: 10.1039/x0xx00000x

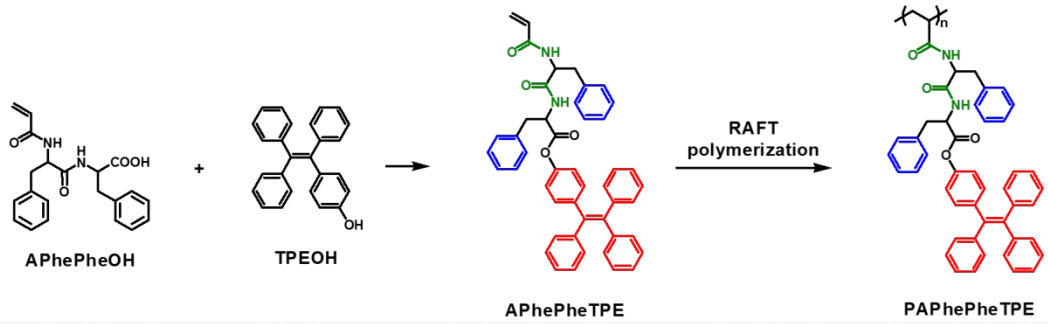

Scheme 1 Synthesis of a diphenylalanine–TPE hybrid monomer (APhePheTPE) and the corresponding hybrid homopolymer (PAPhePheTPE) via reversible addition-fragmentation chain-transfer (RAFT) polymerization.

the fabrication of nano- and microstructures with tunable size/shape and fluorescent properties, which have great potential for applications in devices and sensors.[31-46] Several synthetic approaches have been developed, which include the chemical linkage of AIE molecules with self-assembling motifs,[31-41] conjugation with chiral polymers,[42-44] and co-assembly of AIE molecules and self-assembling motifs.[45,46] The synthesized structures are mainly constructed via non-covalent bonds such as hydrogen bonding, hydrophobic and electrostatic interactions.[32-37,39-41,43-46] As a self-assembling motif, TPE molecules hybridized with amino acids or peptides show the ability to self-assemble into various structures, such as spheres, vesicles, and helical nano- and microfibers, which is achieved through specific interactions derived from amino acids or peptides.[32,33,35,40,41] These hybrid materials also exhibit aggregation-induced circular dichroism (AICD)[32,33,35,43,44] and circularly polarized luminescence due to the transfer of chirality by amino acids to achiral AIE molecules.[32-37,39-41,43,44]

Herein, we report the synthesis, self-assembly, and polymerization of a diphenylalanine–TPE hybrid monomer (APhePheTPE) consisting of diphenylalanine as the self-assembling motif and TPE as an AIE luminogen (AIEgen). Diphenylalanine-containing acrylamide (APhePheOH) bearing a carboxylic acid was combined with the TPE derivative (TPEOH) via condensation to afford a hybrid monomer (APhePheTPE), which was used for the controlled synthesis of the hybrid homopolymer (PAPhePheTPE), as shown in Scheme 1. Scanning electron microscopy (SEM), atomic force microscopy (AFM), circular dichroism (CD), and fluorescence measurements were performed to evaluate the formation of the assembled structures of the APhePheTPE and PAPhePheTPE in selected solvents and their luminescence behavior upon assembly. To the best of our knowledge, the present study is the first to show APhePheTPE as a successful combination of a dipeptide motif involving a polymerizable vinyl group with an AIE unit and the controlled synthesis of the corresponding APhePheTPE, offering the ability to self-assemble into helical nanoribbons, fiber-like and rod-shaped structures, and nanofibers with characteristic AIE and AICD properties.

Results and discussion

Synthesis and characterization of APhePheTPE

A diphenylalanine–TPE hybrid monomer (APhePheTPE) was synthesized via esterification of *N*-acryloyl-L,L-diphenylalanine (APhePheOH)[16] with TPEOH[47] to achieve potential synergistic effect of combining self-assembly of dipeptide and AIE properties. The synthesis was conducted in the presence of *N,N'*-dicyclohexylcarbodiimide and 4-dimethylaminopyridine in tetrahydrofuran (THF), followed by column purification, affording APhePheTPE in 49% yield. The formation of APhePheTPE was confirmed using ^{1}H nuclear magnetic resonance (NMR), which showed the peaks of the vinyl group at 6.22–6.14 and 5.97–5.49 ppm, two amide groups at 8.75 and 8.28 ppm, and phenyl groups from PhePhe and TPE units at 7.24–6.64 ppm (Figure S1). Structural analysis was also performed using ^{13}C NMR (Figure S2), elemental analysis, and 2D NMR (Figures S3 and S4), confirming the synthesis of APhePheTPE. The resulting APhePheTPE exhibited good solubility in organic solvents, such as dimethyl sulfoxide (DMSO), dimethylformamide (DMF), and THF and was soluble in alcoholic solvents (methanol and ethanol) under dilute conditions (less than 10 mM) but insoluble in water (Table S1).

Self-assembly of APhePheTPE

Next, APhePheTPE was used as a self-assembly directing motif to manipulate the formation of the desired assemblies with environmentally sensitive emissions. One of the representative strategies to provide the unique self-assembly of diphenylalanine derivatives is the use of specific solvents with different polarities and suitable concentrations.[6,16,48] In this study, THF and water were selected as the good and poor solvents, respectively (Table S1). First, APhePheTPE was dissolved in THF to obtain the stock solution, which was then diluted with water to obtain the desired THF/water mixtures at arbitrary compositions and concentrations; the mixed solution was allowed to equilibrate for 24 h in all the cases. The SEM images of APhePheTPE nanostructures prepared in THF/water mixtures with different water fractions are illustrated in Figure 1. In the THF/water mixture (10/90 vol%, conc. = 1.0 mg/mL), APhePheTPE self-assembled mainly into right-hand helical nanoribbons. The helical pitch of the nanoribbon was 120 nm and longer, with a relatively constant width of approximately 50 nm (Figures 1a and b); twisted nanofibers and plate-like crystals were also observed occasionally (Figure S5). AFM images also revealed fiber-like structures (Figure S6) that were formed during the evaporation of the THF/water mixture onto the mica

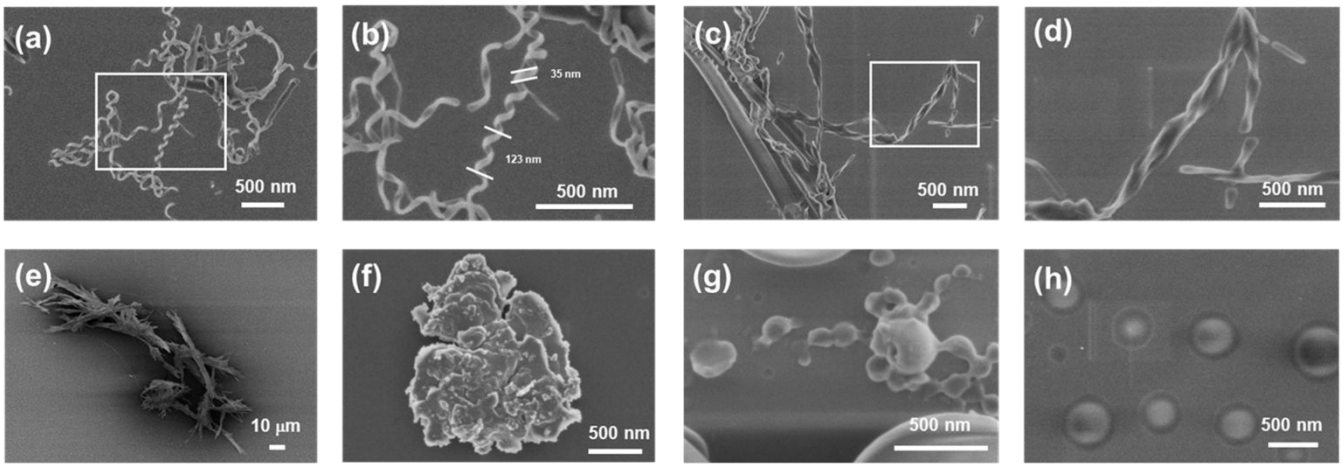

Fig. 1 SEM images showing self-assembled structures of APhePheTPE prepared in THF/water mixtures with different water fractions: (a, b) 90%, (c, d) 80%, (e) 70%, (f) 60%, (g) 30%, and (h) 0% (conc. = 1.0 mg/mL). (b, d) Magnified SEM images of the region inside the box in (a and c).

substrate, which may affect the nucleation growth mechanism.[6] Similar helical nanostructures were observed in SEM images even when the samples were prepared at higher (10.0 mg/mL) and lower (0.03 mg/mL) concentrations in the THF/water (10/90 vol%, Figure S10), suggesting a limited impact of concentration on the assembled structures. The helical nanostructures were partially observed in the system with an 80% water fraction, in addition to the fiber-like structures (Figures 1c and d). The fiber-like structures were predominantly observed at 70% water fraction, and a further decrease in the water fraction led to a structural change from aggregates to large spheres (60, 30, and 0%, Figures 1e–h). AFM images of APhePheTPE samples prepared by drop-casting from THF/water mixtures (20/80 and 30/70 vol%) also indicated the formation of large fiber-like structures (Figures S7 and S8). However, the sample prepared by spin-coating from THF/water mixture (10/90 vol%) showed only small spherical aggregates, which may be attributed to collapse and/or aggregate of nanostructures during rapid solvent evaporation by spin coating (Figure S9). These results suggest that the observed AFM images

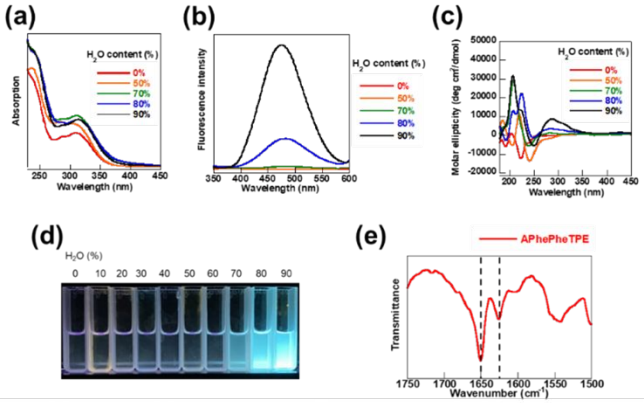

Fig. 2 (a) UV-vis, (b) fluorescence (λ_{ex} = 310 nm), (c) CD spectra of APhePheTPE dissolved in THF and self-assembled in THF/water mixtures (conc. = 0.03 mg/mL). (d) Photographs of luminescence behaviors of APhePheTPE in THF/water mixtures under UV light irradiation (conc. = 0.03 mg/mL, λ_{ex} = 360 nm). (e) FT-IR spectrum of APhePheTPE.

are affected by the sample preparation procedure and conditions. Nevertheless, both AFM and SEM images showed the morphologies transitions, depending on the water fraction in THF/water mixtures. In the DMF/water and THF/MeOH mixtures (10/90 vol%, conc. = 1.0 mg/mL), isolated rod-shaped assemblies and large aggregates consisting mainly of fibers were observed in SEM images (Figures S11 and S12). Water is a poor solvent for APhePheTPE, while the two amide groups and an ester group present within the hybrid monomer contribute to hydrogen bonding. Hence, in the THF/water mixtures, the diphenylalanine unit with amide groups is located on the surface of the assembled states, and the more hydrophobic TPE unit is concentrated in the core, as illustrated in Figure 3a, b. This exposure of the relatively hydrophilic diphenylalanine unit with specific non-covalent interactions is predominant at high water fractions, affording nanoribbon structures. This observation is consistent with that of TPE–amino acid derivatives, in which the co-existence of poor solvent cooperates with hydrogen bonds derived from amino acid moieties to stabilize the helically assembled structures.[38] For comparison, the self-assembly of APhePheOH with a less bulky carboxylic acid, instead of the TPE unit in APhePheTPE, was evaluated, which showed straight nanofibers and bundle structures under the same conditions (THF/water = 10/90 vol%, conc. = 1.0 mg/mL, Figure S13). These results suggest that the diphenylalanine motif chemically linked to the TPE unit imparts a unique self-assembly behavior, thus forming helical nanostructures depending on the solvent polarity.

AIE and chiroptical properties of APhePheTPE

Ultraviolet–visible (UV–vis) absorption and fluorescence measurements were conducted in THF and THF/water mixtures to gain insight into the AIE properties and their correlation with the self-assembly of APhePheTPE. As shown in Figure 2a, APhePheTPE dissolved in THF exhibited absorptions at 240 and 310 nm, corresponding to the phenyl rings of the diphenylalanine and TPE moieties, respectively. When APhePheTPE was excited at 310 nm, the hybrid monomer was almost non-emissive in THF and THF/water mixtures with water

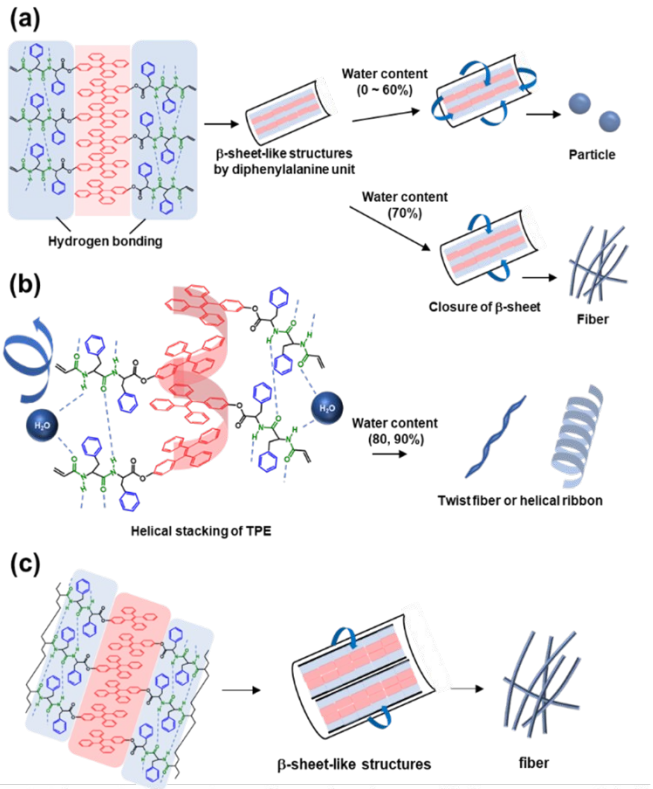

Fig. 3 Schematic illustrations of postulated assembled structures of (a,b) APhePheTPE in THF/water mixtures with different water fractions: (a) 0–70% and (b) 80 and 90%, and (c) PAPhePheTPE in THF/water mixture (10/90 %).

fractions less than 60%, suggesting to non-radiative relaxation via intramolecular rotation of the TPE unit. However, a blue fluorescence with a maximum emission was detected a 475 nm for at a higher water fraction (70%), which corresponded to the AIE phenomenon originating from the aggregation of TPE units (Figures 2b and d). The highest fluorescence intensity of APhePheTPE was obtained for the mixture with the highest water fraction (90%). Hence, the change in the water fraction of the THF/water mixtures is an essential factor in manipulating the fluorescence properties and assembled structures of the diphenylalanine–TPE hybrid monomer. Thus, stronger emissions are achieved as a higher content of poor solvent (water) leads to remarkable aggregation of the TPE units in the helical nanoribbons and fiber-like structures.

CD measurements were performed to investigate the chiroptical properties of the diphenylalanine–TPE hybrid monomer. Diphenylalanine shows characteristic positive Cotton effects at approximately 200 and 220 nm, which were attributed to the n–π* and π–π* transitions derived from hydrogen bonding and the π–π stacking interactions of diphenylalanine with the β-sheet structures.[4,17,49] As shown in Figures 2c and S14, APhePheTPE exhibited no characteristic positive Cotton effect in the THF solution, and a strong negative peak was visible at 220 nm. However, the intensity of the negative peak decreased with an increase in water content. Furthermore, positive Cotton effects at approximately 200 and 220 nm due to the n–π* and π–π* transitions, as well as a new Cotton effect at 280–350 nm were detected when the water fraction in the THF/water mixtures reached 80%, which corresponded to the AICD phenomenon (Figure 2c).[32,33,35,43,44]The broad CD peak at 280–350 nm was attributed to the helical stacking of the TPE unit via chiral transfer from amino acid moieties to the TPE units in various amino acid–TPE conjugates.[32,33,44] Similar enhancement of CD by aggregation (AICD) was also reported in other systems.[50,51] When the water fraction in the THF/water mixture was varied to 90%, a further increase was observed in the TPE-derived peak at 280–350 nm (Figures S14 and S15), suggesting that the transformation of the APhePheTPE-assembled structures into helical nanoribbons is related to the AICD property.

Fourier transform infrared (FT-IR) measurements were also conducted to evaluate the intramolecular interactions of monomeric APhePheTPE, which showed two amide absorptions at 1625 cm^{-1} and 1650 cm^{-1} (Figure 2e). The peak at 1625 cm^{-1} is attributed to β-sheet structures,[52] which may be related to the TPE-induced diphenylalanine unit, because APhePheOH used for comparison showed only the peaks corresponding to β-turns (1648 cm^{-1} and 1670 cm^{-1}, Figure S16).[49,53] A peak corresponding to the α-helix conformation was detected at approximately 1660 cm^{-1},[51] which may have overlapped with the strong peak at 1650 cm^{-1} in APhePheTPE. The peak at approximately 1650 cm^{-1}, which was visible in APhePheTPE and APhePheOH, is attributed to the hydrogen-bonded β-sheet conformation with antiparallel configurations[6] or aperiodic secondary structures.[49]

From these results, as illustrated in Figure 3, parallel stacking via hydrogen bonding and π–π stacking derived from diphenylalanine is predominant at low water fractions (0–70%) in THF/water mixtures. By increasing the water fraction (80%), this stacking is transformed into the helical stacking of the TPE moiety, resulting in thermodynamically stable nanostructures, such as helical and twisted structures. This behavior is related to two coexisting mechanisms derived from diphenylalanine derivatives[1,2] and TPE–amino acid amphiphiles,[41] which includes several steps: (1) formation of bilayered assemblies consisting of antiparallel-arranged APhePheTPE via stacking interactions between the diphenylalanine-based aromatic moieties, π–π interactions of TPE units, and intra- and intermolecular amide-based hydrogen bonds; (2) formation of extended sheets via stabilization by aromatic interactions and hydrogen bonds, and (3) formation of helical nanoribbons, fiber-like structures, and large spheres, depending on the nature of the monomeric diphenylalanine–TPE hybrid (APhePheTPE) and sample preparation conditions (such as the THF/water ratios). The mechanism of the second step is similar to that of the self-assembly process of diphenylalanine derivatives involving sheet formation, followed by rolling up.[2] The first and third steps rely on the unique structures of the diphenylalanine–TPE hybrid.[41]

Table 1 RAFT polymerization of APhePheTPE using a trithiocarbonate-type chain transfer agent (CTA) [a]

Run	[APhePheTPE]/ [CTA]/[AIBN]	Conv.[b] /Yield[c] (%)	M_n[d] (theory)	M_n[b] (NMR)	M_n[e] (SEC)	M_w/M_n[e] (SEC)
1	20/2/1	83/71	6000	7600	4600	1.40
2	50/2/1	76/48	13200	14800	9300	1.34
3	100/2/1	64/41	22600	24100	12000	1.27

[a] Polymerization in dimethylformamide (DMF; conc. = 0.20 g/mL) at 60 °C for 24 h. [b] Calculated using ^{1}H NMR in dimethyl sulfoxide (DMSO)-d_6. [c] Diethylether-insoluble part. [d] Theoretical molecular weight ($M_{n,\ theory}$) = (MW of APhePheTPE) × ([APhePheTPE]$_0$/[CTA]$_0$) × conv. + (MW of CTA). [e] Determined by size-exclusion chromatography (SEC) in DMF (0.01 M LiBr)

The dynamic morphological transition of APhePheTPE with changes in the emission properties was investigated in THF/water mixtures (10/90, 20/80, and 30/70 vol%). When the THF stock solution was added to water, a slightly turbid dispersion was obtained in the THF/water mixture (10/90, conc. = 1.0 mg/mL), which changed to floating assembled structures. A gradual change from a turbid dispersion to a precipitated assembled structure was also observed in THF/water (10/90, 0.03 mg/mL) mixture. A similar time-dependent change was previously reported for functionalized diphenylalanine derivatives.[7] For instance, fluorenyl-9-methoxy carbonyl diphenylalanine in DMSO reportedly undergoes rapid precipitation when water is added, followed by a change from an opaque white mixture to a clear gel within 5 min.[54,55] In the system of our study, several microcrystals were predominantly detected in the SEM image (Figure S17) immediately after mixing the APhePheTPE THF solution with water, which is distinct from the nanoribbons (Figures 1a and b) observed after equilibration for 24 h. This implies a gradual structural transformation of the microcrystals into nanoribbons in the THF/water (10/90, 1.0 mg/mL) mixture. The time-dependent UV–vis and fluorescence spectra of APhePheTPE in the THF/water mixture (conc. = 0.03 mg/mL) indicated gradual changes in the absorption and emission peak intensities, with slight peak shifts until 24 h (Figure S18). The absorption of APhePheTPE decreased over time, probably owing to the transformation from small assemblies into larger microscopic clusters and/or assembled structures, similar to other systems.[56,57] Furthermore, a slight increase in fluorescence intensity was detected, with a blue-shifted peak from 475 nm to 452 nm. In the normalized UV-vis spectra (Figure S18b), the absorbance derived from TPE unit was also blue shifted from 314 nm to 308 nm, suggesting the possibility to form APhePheTPE H-aggregates by TPE core units with alignment, as illustrated in Figure 3b. Similar H-type helical structures were also reported in other systems.[58-62] CD measurements indicated an apparent decrease in the peaks attributed to diphenylalanine at 200 and 220 nm, with an increase in the peak attributed to the TPE unit at 280–350 nm as the self-assembly progressed up to 24 h. This result suggested a structural change from β-sheet-rich plane to a helical structure in the THF/water (10/90) mixture.

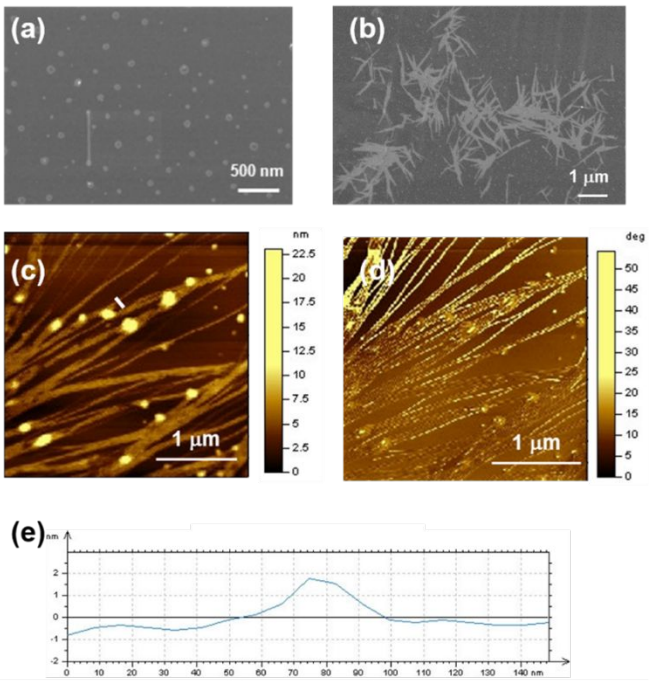

Fig 4. SEM images showing (a) sphere- and (b) acicular -like structures, and AFM (c) height and (d) phase images showing nanofibers derived from PAPhePheTPE (M_n = 24100, Mw/M_n = 1.27) in (a) THF and (b-d) THF/water mixture (10/90 vol%). Conc. = (a, c-d) 1.0 mg/mL and (b) 0.03 mg/mL. (e) cross section at the position indicated by the white line in (c).

Similar time-dependent changes were observed in the absorption, fluorescence, and CD peaks in THF/water mixtures (30/70 and 20/80 vol%) (Figures S19 and S20). Interestingly, the samples prepared immediately after mixing the APhePheTPE THF solution with water exhibited low fluorescence intensity, which strongly increased with time. The relationship between emission in solution/suspension states and morphological transition observed by SEM measurement are shown in Figure S21. When the samples were prepared immediately after THF/water mixing (30/70, 20/80, and 10/90 vol%), sphere-, plate- and short nanofiber-like structures were observed with relatively low emission. After 3 h, morphological changes into microcrystal, nanofibers, nanoribbons were observed in SEM images with higher emissions in suspension states, suggesting that the change in the fluorescence intensity is related closely to the morphological transition. Large assembled objects obtained from APhePheTPE monomer in THF/water mixtures can be dispersed, depending on the THF/water ratios, while APhePheTPE behaves as single dissolved molecules or small assemblies to afford transparent solutions in THF. Obviously, large objects having the sizes of hundreds of nanometers to a few micrometer should affect the reflection of light and absorbance, resulting in the different emission behaviors.

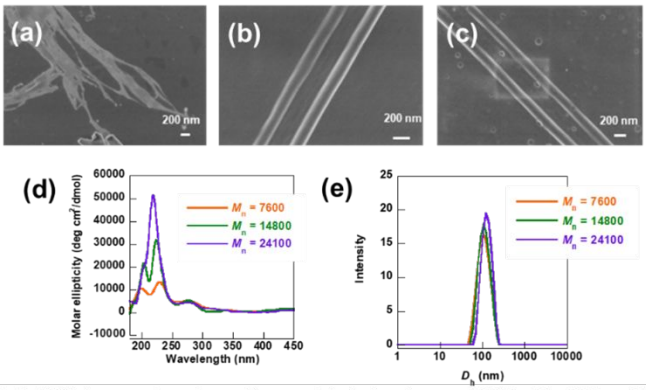

Fig 5. SEM images showing self-assembled structures of PAPhePheTPEs with different molecular weights, M_n = (a) 7600, (b) 14800, and (c) 24100, in the THF/water mixture (10/90 vol%, conc. = 1.0 mg/mL). (d) CD spectra and € DLS traces of PAPhePheTPEs in the THF/water mixture (10/90 vol%, conc. = 0.03 mg/mL).

Similar fluorescence change ascribed to the time-dependent morphological transition was observed in another AIE molecule.[63] In the THF/water (20/80) mixture, a broad positive CD peak corresponding to the TPE-derived Cotton effect was still visible, whereas the TPE-derived Cotton effect disappeared in the THF/water (30/70) mixture, implying the disappearance of the helical structure with decreasing water fraction. This tendency is consistent with the assembled structures detected by SEM (Figures 1a–e), showing helical nanoribbons (10/90), helical nanostructures with fiber-like structures (20/80), and fiber-like structures (30/70) in the THF/water mixtures.

Polymerization of APhePheTPE

Diphenylalanine–TPE hybrid homopolymer (PAPhePheTPE) bearing a bulky side chain consisting of diphenylalanine with the self-assembling ability and TPE with AIE properties were synthesized via RAFT polymerization (Scheme 1). RAFT polymerization of APhePheTPE was conducted in DMF at 60 °C in the presence of azobisisobutyronitrile (AIBN) as initiator at [chain transfer agent $[CTA]_0/[AIBN]_0$ = 2 using a trithiocarbonate-type CTA. As shown in Table 1, the polymerization at $[APhePheTPE]_0/[CTA]_0/[AIBN]_0$ = 20/2/1 afforded a polymer in 71% yield. The structure of the resulting PAPhePheTPE was confirmed using ^{1}H NMR and 2D NMR spectroscopy in DMSO-d_6 (Figures S22a and S23). The DMF size-exclusion chromatography (SEC; 10 mM LiBr) of PAPhePheTPE revealed relatively low dispersity (M_w/M_n = 1.40) and reasonable molecular weights of $M_{n,SEC}$ = 4,600 and $M_{n,NMR}$ = 7,600, which are comparable to the theoretical value (M_n = 6000) calculated from the monomer conversion and monomer-to-CTA molar ratio in the feed.

RAFT polymerization at higher $[APhePheTPE]_0/[CTA]_0$ molar ratios (20 and 50) was conducted under the same conditions to synthesize APhePheTPEs with longer chain lengths. Unimodal SEC peaks were observed for the resulting PAPhePheTPEs, which shifted toward higher molecular weights with increasing $[APhePheTPE]_0/[CTA]_0$ ratios (Figure S22b). The increase in the M_n of the PAPhePheTPEs while maintaining low polydispersities ($M_{n,NMR}$ = 14800–24100, M_w/M_n = 1.34–1.27) and sufficient polymer yields suggests the feasibility of tuning the chain lengths of the diphenylalanine–TPE hybrid homopolymers. When the polymerization was conducted at $[CTA]_0/[I]_0$ = 5 and 10, however, a remarkable decrease in the polymer yield was observed (Table S2), which is probably due to relatively low reactivity of APhePheTPE originated from bulky side chain. Similar to monomeric APhePheTPE, PAPhePheTPE was soluble in DMSO and THF but insoluble in water, which imparts the AIE property of PAPhePheTPE in mixed solvents.

Self-assembly and luminescence behavior of PAPhePheTPE

The self-assembled structures of PAPhePheTPE were prepared from THF/water mixtures under the same conditions as those used for the self-assembly of monomeric APhePheTPE. As shown in Figure 4b, an acicular structure was predominantly obtained when the PAPhePheTPE sample (M_n = 24100) was prepared from dilute THF/water (10/90 vol%, 0.03 mg/mL) mixture. In contrast, a higher concentration (1.0 mg/mL) led to the formation of rod-shaped structures and nanofibers, as confirmed by the SEM and AFM measurements (Figures 4c–e). The AFM height image suggested that the nanofibers had a persistence length on the order of micrometers, approximately 2 nm in height and 50 nm in width (Figure 4e). AFM analysis indicated the existence of stable fiber-like structures that were absorbed on the mica surface in a hydration environment. Gazit et al. demonstrated a fast-evaporation-indicated self-assembly of dipeptide on the solid phase.[64] In our system, rapid evaporation of THF from THF/water mixtures may occur owing to the lower boiling point of THF compared to that of water, contributing to forming fiber-like assembled structures on the mica surface. Spherical morphologies were observed in the SEM image of the sample prepared from a non-selective THF solution (Figure 4a). Unlike APhePheTPE, no helical nanostructure was

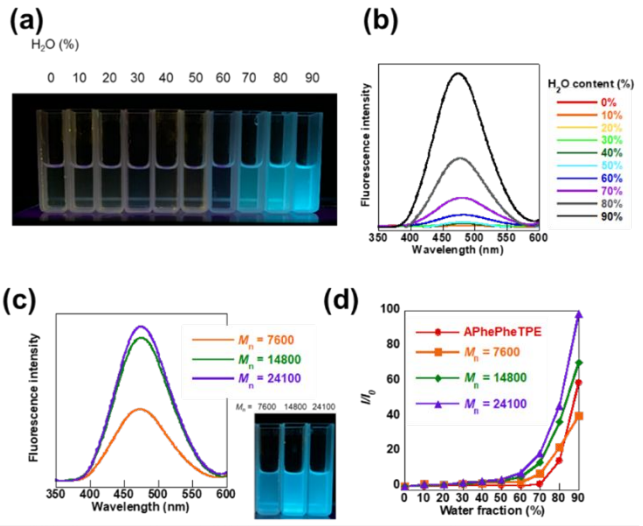

Fig. 6 (a) Photograph and (b) fluorescence spectra of PAPhePheTPE (M_n = 24100, M_w/M_n = 1.27) in THF/water mixtures. (c) M_n–dependent fluorescence spectra of PAPhePheTPEs in the THF/water (10/90) mixture (conc. = 0.03 mg/mL). (d) Plots of emission peak intensity (I/I_0) at 475 nm against the water fraction of the THF/water mixtures, where I = peak intensity and I_0 = peak intensity in pure THF.

detected for PAPhePheTPE, suggesting that the formation of a carbon–carbon main chain from the vinyl group may interfere specific interactions to form unique helical structures of monomeric APhePheTPE.

The effect of the molecular weight of PAPhePheTPEs on the assembled structures and AIE behavior was evaluated (Figures 5 and 6). The CD spectra of PAPhePheTPE (M_n = 14800) in the THF/water mixture (10/90 vol%) exhibited strong positive peaks at 200 nm and 220 nm. The intensity of the positive peak at 220 nm increased with increasing molecular weight, suggesting an increase in the stacking interactions between the diphenylalanine-based aromatic rings (Figure 5d). The positive Cotton effect at 280–350 nm originating from the TPE moiety was still visible, implying that the chirality transformation from the diphenylalanine into TPE moieties remained in the polymeric states, with the preservation of the AICD property. This remarkable increase in the positive Cotton effect attributed to the π–π interaction of the diphenylalanine unit with a weak TPE-based peak suggests the preferable formation of rod-shaped structures with increasing molecular weights of PAPhePheTPEs; the phenomenon is consistent with the tendency observed in the SEM images (Figures 5a–c). This structural transition is distinct from that of monomeric APhePheTPE and PAPhePheOH used for comparison (Figures S24 and S25). Dynamic light scattering (DLS) measurements showed a unimodal peak corresponding to the assembled structure (D_h = 100–120 nm, Figure 5e) independent of the molecular weight of PAPhePheTPE. FT-IR measurements of PAPhePheTPEs showed a broad peak in the range of 1600–1700 cm^{-1} (Figure S26), and clear absorptions corresponding to β-sheet conformations (1625 and 1650 cm^{-1} observed in the monomeric APhePheTPE) were difficult to detect, regardless of the molecular weight. Nevertheless, the SEM and CD measurement results suggest that PAPhePheTPEs form β-sheet-like structures induced by hydrogen bonds and π–π interactions of diphenylalanine, subsequently forming a fibrous structure via the closing of the β sheets (Figure 3c).[2]

The UV–vis spectrum of PAPhePheTPE showed absorbance at approximately 250 and 310 nm, and blue fluorescence with a maximum emission at 475 nm was detected in THF/water (10/90, Figures 6a and b), which are almost comparable to those of monomeric APhePheTPE. As shown in Figure 6a, PAPhePheTPE was vertically nonluminescent in the molecularly dissolved state in THF and THF/water mixtures with water fractions less than 60%, whereas a remarkable emission was detected in 70% water fractions. The emission was stronger as the water fraction increased on the THF/water mixtures, whereas no significant shift was observed in the fluorescence spectra (Figures 6b and S27), which is distinct from the tendency of monomeric APhePheTPE. Because water is a poor solvent for PAPhePheTPE, the hybrid homopolymer chain aggregated in THF/water mixtures with high water fractions. Interestingly, PAPhePheTPEs showed strong emission with increasing molecular weight (Figure 6c), indicating that the diphenylalanine- and TPE-derived interactions concertedly affected the aggregation states and restricted intramolecular rotation of the TPE moiety. The quantum yields of APhePheTPE monomer and homopolymers in THF/water mixture (10/90-vol%) were approximately 7–12% (Table S3). The fluorescence intensity and I/I_0 were plotted against the water fraction in the THF/water mixtures (Figure 6d). PAPhePheTPE with the highest molecular weight displayed a remarkable increase in luminescence against the water fraction, whereas a low-molecular-weight PAPhePheTPE resulted in lower water (a poor solvent)-induced luminescence.

Conclusion

In this study, we developed a diphenylalanine–TPE hybrid monomer (APhePheTPE) by covalently linking diphenylalanine-containing acrylamide with a TPE unit. The hybrid monomer can self-assemble into various nano/microstructures with characteristic AIE and AICD properties. Depending on the water fraction, the assembled structures from monomeric APhePheTPE in THF/water mixtures undergo a morphological transition from large spheres, nano/micro fiber-like structures, and nanoribbons. In particular, the AIE and AICD properties are correlated with the assemblies of APhePheTPE, which facilitates structural design suitable for desired chiral fluorescent materials in selective solvents. PAPhePheTPE exhibited unique molecular weight-dependent AIE and AICD properties, which increased the emission and CD peak intensities with increasing molecular weight. The understanding and manipulation of the precise nature of hydrophobic interactions and hydrogen bonds in the hybrid monomer and corresponding polymer can facilitate the future development of bio-inspired nanomaterials, sensing, and optoelectronic materials.

Author contributions

Ryo Yonenuma: Investigation, Methodology, Writing- original draft. Hideharu Mori: Conceptualization, Supervision, Validation, Writing-review & editing.

Conflicts of interest

There are no conflicts to declare.

Acknowledgements

This work was supported by JST, the establishment of university fellowships towards the creation of science technology innovation, Grant Number JPMJFS2104.

Notes and references

1. M. Reches and E. Gazit, *Science*, 2003, **300**, 625-627.
2. M. Reches and E. Gazit, *Nano Lett.*, 2004, **4**, 581-585.
3. J. Kim, T. H. Han, Y. I. Kim, J. S. Park, J. Choi, D. G. Churchill, S. O. Kim and H. Ihee, *Adv. Mater.*, 2010, **22**, 583-587.

4. L. Adler-Abramovich, M. Reches, V. L. Sedman, S. Allen, S. J. B. Tendler and E. Gazit, *Langmuir*, 2006, **22**, 1313-1320.
5. T. H. Han, J. Kim, J. S. Park, C. B. Park, H. Ihee and S. O. Kim, *Adv. Mater.*, 2007, **19**, 3924-3927.
6. P. Zhu, X. Yan, Y. Su, Y. Yang and J. Li, *Chem. - Eur. J.*, 2010, **16**, 3176-3183.
7. N. A. Dudukovic and C. F. Zukoski, *Langmuir*, 2014, **30**, 4493-4500.
8. V. Nguyen, R. Zhu, K. Jenkins and R. Yang, *Nat. Commun.*, 2016, **7**, 13566.
9. S. Safaryan, V. Slabov, S. Kopyl, K. Romanyuk, I. Bdikin, S. Vasilev, P. Zelenovskiy, V. Y. Shur, E. A. Uslamin, E. A. Pidko, A. V. Vinogradov and A. L. Kholkin, *ACS Appl. Mater. Interfaces*, 2018, **10**, 10543-10551.
10. S. L. Porter, S. M. Coulter, S. Pentlavalli, T. P. Thompson and G. Laverty, *Acta Biomater*, 2018, **77**, 96-105.
11. Y. C. Tsai, C. C. Tang, H. H. Wu, Y. S. Wang and Y. F. Chen, *Int. J. Pept. Res. Ther.*, 2019, **26**, 1107-1114.
12. M. Yemini, M. Reches, J. Rishpon and E. Gazit, *Nano Lett.*, 2005, **5**, 183-186.
13. M. Yemini, M. Reches, E. Gazit and J. Rishpon, *Anal. Chem.*, 2005, **77**, 5155-5159.
14. H. Skaat, R. Chen, I. Grinberg and S. Margel, *Biomacromolecules*, 2012, **13**, 2662-2670.
15. H. A. Kim, H. J. Lee, J. H. Hong, H. J. Moon, D. Y. Ko and B. Jeong, *Biomacromolecules*, 2017, **18**, 2214-2219.
16. R. Yonenuma, A. Ishizuki, K. Nakabayashi and H. Mori, *J. Polym. Sci., Part A: Polym. Chem.*, 2019, **57**, 2562-2574.
17. J. L. Warren, P. A. Dykeman-Bermingham and A. S. Knight, *J. Am. Chem. Soc.*, 2021, **143**, 13228-13234.
18. S. K. Murase, N. Haspel, L. J. del Valle, E. A. Perpète, C. Michaux, R. Nussinov, J. Puiggalí and C. Alemán, *RSC Adv.*, 2014, **4**, 23231-23241.
19. E. Mayans, S. K. Murase, M. M. Pérez-Madrigal, C. Cativiela, C. Alemán and J. Puiggalí, *Macromol. Chem. Phys.*, 2018, **219**, 1800168.
20. F. Zhang, R. Wang, Y. He, W. Lin, Y. Li, Y. Shao, J. Li, M. Ding, F. Luo, H. Tan and Q. Fu, *J. Mater. Chem. B*, 2018, **6**, 4326-4337.
21. C. J. Kim, J. E. Park, X. Hu, S. K. Albert and S. J. Park, *ACS Nano*, 2020, **14**, 2276-2284.
22. T. P. T. Dao, L. Vezenkov, G. Subra, M. Amblard, M. In, J.-F. Le Meins, F. Aubrit, M.-A. Moradi, V. Ladmiral and M. Semsarilar, *Macromolecules*, 2020, **53**, 7034-7043.
23. T. P. T. Dao, L. Vezenkov, G. Subra, V. Ladmiral and M. Semsarilar, *Polym. Chem.*, 2021, **12**, 113-121.
24. Y. Hong, J. W. Y. Lam and B. Z. Tang, *Chem. Soc. Rev.*, 2011, **40**, 5361-5388.
25. J. Luo, Z. Xie, J. W. Y. Lam, L. Cheng, H. Chen, C. Qiu, H. S. Kwok, X. Zhan, Y. Liu, D. Zhu and B. Z. Tang, *Chem. Commun.*, 2001, **18**, 1740-1741.
26. X. Cai and B. Liu, *Angew. Chem. Int. Ed. Engl.*, 2020, **59**, 9868-9886.
27. Q. Wan, Q. Huang, M. Liu, D. Xu, H. Huang, X. Zhang and Y. Wei, *Appl. Mater. Today*, 2017, **9**, 145-160.
28. R. Hu, A. Qin and B. Z. Tang, *Prog. Polym. Sci.*, 2020, **100**, 101176.
29. S. Xie, A. Y. H. Wong, R. T. K. Kwok, Y. Li, H. Su, J. W. Y. Lam, S. Chen and B. Z. Tang, *Angew. Chem. Int. Ed. Engl.*, 2018, **57**, 5750-5753.
30. A. Qin, J. W. Y. Lam, L. Tang, C. K. W. Jim, H. Zhao, J. Sun and B. Z. Tang, *Macromolecules*, 2009, **42**, 1421-1424.
31. S. Zhang, J. M. Yan, A. J. Qin, J. Z. Sun and B. Z. Tang, *Chin. Chem. Lett.*, 2013, **24**, 668-672.
32. H. Li, J. Cheng, Y. Zhao, J. W. Y. Lam, K. S. Wong, H. Wu, B. S. Li and B. Z. Tang, *Mater. Horiz.*, 2014, **1**, 518-521.
33. H. Li, X. Zheng, H. Su, J. W. Y. Lam, K. Sing Wong, S. Xue, X. Huang, X. Huang, B. S. Li and B. Z. Tang, *Sci. Rep.*, 2016, **6**, 19277.
34. H. Li, S. Xue, H. Su, B. Shen, Z. Cheng, J. W. Lam, K. S. Wong, H. Wu, B. S. Li and B. Z. Tang, *Small*, 2016, **12**, 6593-6601.
35. B. S. Li, R. Wen, S. Xue, L. Shi, Z. Tang, Z. Wang and B. Z. Tang, *Mater. Chem. Front.*, 2017, **1**, 646-653.
36. G. Huang, R. Wen, Z. Wang, B. S. Li and B. Z. Tang, *Mater. Chem. Front.*, 2018, **2**, 1884-1892.
37. S. P. Goskulwad, M. A. Kobaisi, D. D. La, R. S. Bhosale, M. Ratanlal, S. V. Bhosale and S. V. Bhosale, *Chem. - Asian J.*, 2018, **13**, 3947-3953.
38. B. S. Li, X. Huang, H. Li, W. Xia, S. Xue, Q. Xia and B. Z. Tang, *Langmuir*, 2019, **35**, 3805-3813.
39. S. P. Goskulwad, V. G. More, M. A. Kobaisi, R. S. Bhosale, D. D. La, F. Antolasic, S. V. Bhosale and S. V. Bhosale, *ChemistrySelect*, 2019, **4**, 2626-2633.
40. Y. Shi, G. Yin, Z. Yan, P. Sang, M. Wang, R. Brzozowski, P. Eswara, L. Wojtas, Y. Zheng, X. Li and J. Cai, *J. Am. Chem. Soc.*, 2019, **141**, 12697-12706.
41. Y. Wang, D. Niu, G. Ouyang and M. Liu, *Nat. Commun.*, 2022, **13**, 1710.
42. X. Liu, J. Jiao, X. Jiang, J. Li, Y. Cheng and C. Zhu, *J. Mater. Chem. C*, 2013, **1**, 4713-4719.
43. Q. Liu, Q. Xia, S. Wang, B. S. Li and B. Z. Tang, *J. Mater. Chem. C*, 2018, **6**, 4807-4816.
44. Q. Liu, Q. Xia, Y. Xiong, B. S. Li and B. Z. Tang, *Macromolecules*, 2020, **53**, 6288-6298.
45. Q. Li, J. Zhang, Y. Wang, G. Zhang, W. Qi, S. You, R. Su and Z. He, *Nano Lett.*, 2021, **21**, 6406-6415.
46. J. Li, X. Peng, D. Chen, S. Shi, J. Ma and W. Y. Lai, *ACS Macro Lett.*, 2022, **11**, 1174-1182.
47. A. S. Abd-El-Aziz, C. Agatemor, N. Etkin and B. Wagner, *Macromol. Rapid Commun.*, 2016, **37**, 1235-1241.
48. T. O. Mason, D. Y. Chirgadze, A. Levin, L. Adler-Abramovich, E. Gazit, T. P. J. Knowles and A. K. Buell, *ACS Nano*, 2014, **8**, 1243-1253.
49. M. Gupta, A. Bagaria, A. Mishra, P. Mathur, A. Basu, S. Ramakumar and V. S. Chauhan, *Adv. Mater.*, 2007, **19**, 858-861.
50. J. Kumar, T. Nakashima and T. Kawai, *J. Phys. Chem. Lett.*, 2015, **6**, 3445-3452.
51. Z. Song, H. Sato, A. Pietropaolo, Q. Wang, S. Shimoda, H. Dai, Y. Imai, H. Toda, T. Harada, Y. Shichibu, K. Konishi, M. Bando, N. Naga and T. Nakano, *Chem. Commun.*, 2022, **58**, 1029-1032.
52. C. Tang, A. M. Smith, R. F. Collins, R. V. Ulijn and A. Saiani, *Langmuir*, 2009, **25**, 9447-9453.
53. M. Reches and E. Gazit, *Isr. J. Chem.*, 2005, **45**, 363-371.
54. R. Orbach, L. Adler-Abramovich, S. Zigerson, I. Mironi-Harpaz, D. Seliktar and E. Gazit, *Biomacromolecules*, 2009, **10**, 2646-2651.
55. R. Orbach, I. Mironi-Harpaz, L. Adler-Abramovich, E. Mossou, E. P. Mitchell, V. T. Forsyth, E. Gazit and D. Seliktar, *Langmuir*, 2012, **28**, 2015-2022.
56. H. Nakanishi, A. Deak, G. Hollo and I. Lagzi, *Angew. Chem. Int. Ed. Engl.*, 2018, **57**, 16062-16066.
57. E. M. Kohn, D. J. Shirley, N. M. Hinds, H. C. Fry and G. A. Caputo, *Pept. Sci.*, 2022, **114**, e24288.
58. W. Lv, X. Wu, Y. Bian, J. Jiang and X. Zhang, *Chemphyschem*, 2009, **10**, 2725-2732.

59. C. Zhang, L. Jing, S. Lin, Z. Hao, J. Tian, X. Zhang and P. Zhu, *Chemphyschem*, 2013, **14**, 3827-3833.
60. A. T. Haedler, S. C. Meskers, R. H. Zha, M. Kivala, H. W. Schmidt and E. W. Meijer, *J. Am. Chem. Soc.*, 2016, **138**, 10539-10545.
61. Z. Li, C. J. t. Zeman, S. R. Valandro, J. P. O. Bantang and K. S. Schanze, *J. Am. Chem. Soc.*, 2019, **141**, 12610-12618.
62. R. Zheng, J. Yang, M. Mamuti, D. Y. Hou, H. W. An, Y. Zhao and H. Wang, *Angew. Chem. Int. Ed. Engl.*, 2021, **60**, 7809-7819.
63. T. Ning, L. Liu, D. Jia, X. Xie and D. Wu, *J. Photochem. Photobiol., A*, 2014, **291**, 48-53.
64. M. Reches and E. Gazit, *Nat. Nanotechnol.*, 2006, **1**, 195-200.